Electronic Supplementary Material (ESI) for New Journal of Chemistry.

Supporting Information

Biginelli-based Organic Nanoprobe for Simultaneous Estimation of Tyramine and 1, 2-Diaminopropane: application in real samples.

Gaganpreet Kaur,[a] Tilak Raj,[b] Navneet Kaur[a,c*] and Narinder Singh[b*]

[a]Centre for Nanoscience & Nanotechnology (UIEAST), Panjab University, Chandigarh, 160014, India. E-mail: navneetkaur@pu.ac.in; Tel: +91-1722534464

[b]Department of Chemistry, Indian Institute of Technology Ropar, Rupnagar, Punjab, India, 140001. E-mail: nsingh@iitrpr.ac.in; Fax: +91-1881223395; Tel: +91-1881242176.

[c]Department of Chemistry, Panjab University, Chandigarh, 160014, India. E-mail: navneetkaur@pu.ac.in

Table of contents

Figure S1. ^{1}H NMR spectrum of compound **1** and its expansion.

Figure S2. ^{13}C NMR spectrum of compound **1**.

Figure S3. ESI Mass spectrum of compound **1**.

Figure S4. Plot of variation in size of nanoparticles as a function of concentration of compound **1** in water.

Figure S5. Linear regression graph for Ag (I) titration.

Figure S6. Linear regression graphs for Tyramine titration (A) and linear regression graph for 1,2-Diaminopropane titration (B).

Figure S7. Non-linear regression graphs between Fluorescence Intensity vs. Concentrations of amines (at higher concentrations).

Figure S8. Fluorescence spectra of nano-aggregates **N1** at different concentrations of TBA perchlorate to evaluate the salt effect.

Figure S9. Fluorescence spectra of nano-aggregates **N1** at different pH values.

Figure S10. Fluorescence intensity v/s pH graphs of A) **N1.Ag(I)** complex with 50 µM Tyramine and B) **N1.Ag(I)** complex with 50 µM 1,2-Diaminopropane.

Figure S11. Plot of fluorescence intensity ratios of **N1** and Ag (I) at different concentrations, as a function of time.

Figure S12. Stability of organic nanoparticles, **N1** and the **N1.Ag(I)** complex over a period of two weeks.

Figure S13. Fluorescence intensity variation of A) **N1** on addition of different metal ions and B) **N1.Ag(I)** on addition of different Biogenic amines using five different batches of sensors to check the reproducibility.

Figure S14. Fluorescence intensity variation of A) **N1** on addition of different metal ions and B) **N1.Ag(I)** on addition of different Biogenic amines in presence of HEPES buffer, pH 7.4.

Figure S15. Fluorescence intensity v/s wavelength graph of **N1.Ag(I)** complex with 50 µM each of Tyramine and 50 µM 1, 2-Diaminopropane mixed together.

Table S1: Comparison of current sensor with existing literature.

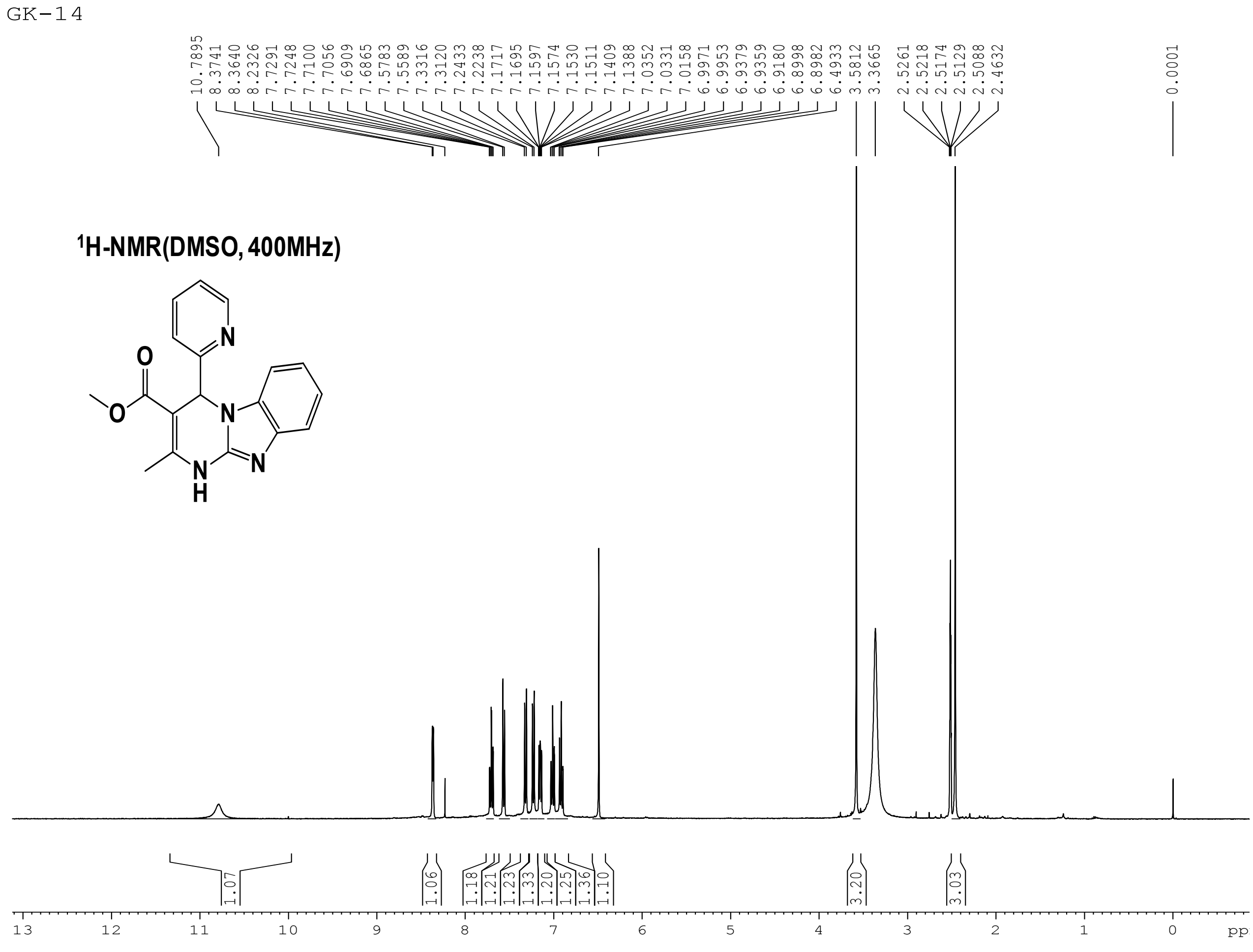
GK-14
^{1}H-NMR(DMSO, 400MHz)
10.7895 8.3741 8.3640 8.2326 7.7291 7.7248 7.7100 7.7056 7.6909 7.6865 7.5783 7.5589 7.3316 7.3120 7.2433 7.2238 7.1717 7.1695 7.1597 7.1574 7.1530 7.1511 7.1409 7.1388 7.0352 7.0331 7.0158 6.9971 6.9953 6.9379 6.9359 6.9180 6.8998 6.8982 6.4933 3.5812 3.3665 2.5261 2.5218 2.5174 2.5129 2.5088 2.4632 0.0001
1.07 1.06 1.18 1.21 1.23 1.33 1.20 1.25 1.36 1.10 3.20 3.03
13 12 11 10 9 8 7 6 5 4 3 2 1 0 pp

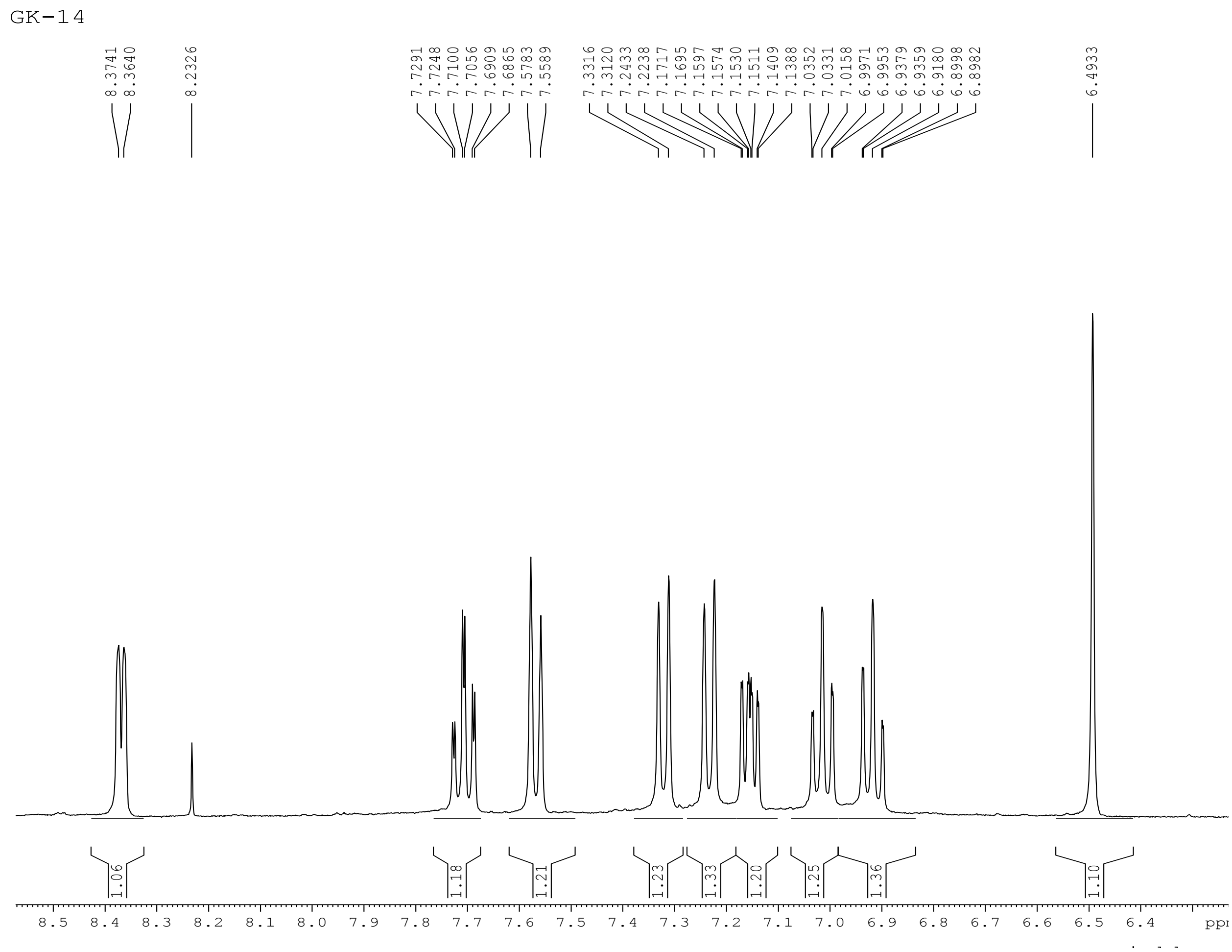

Figure S1. ^{1}H NMR spectrum of compound **1** and its expansion.

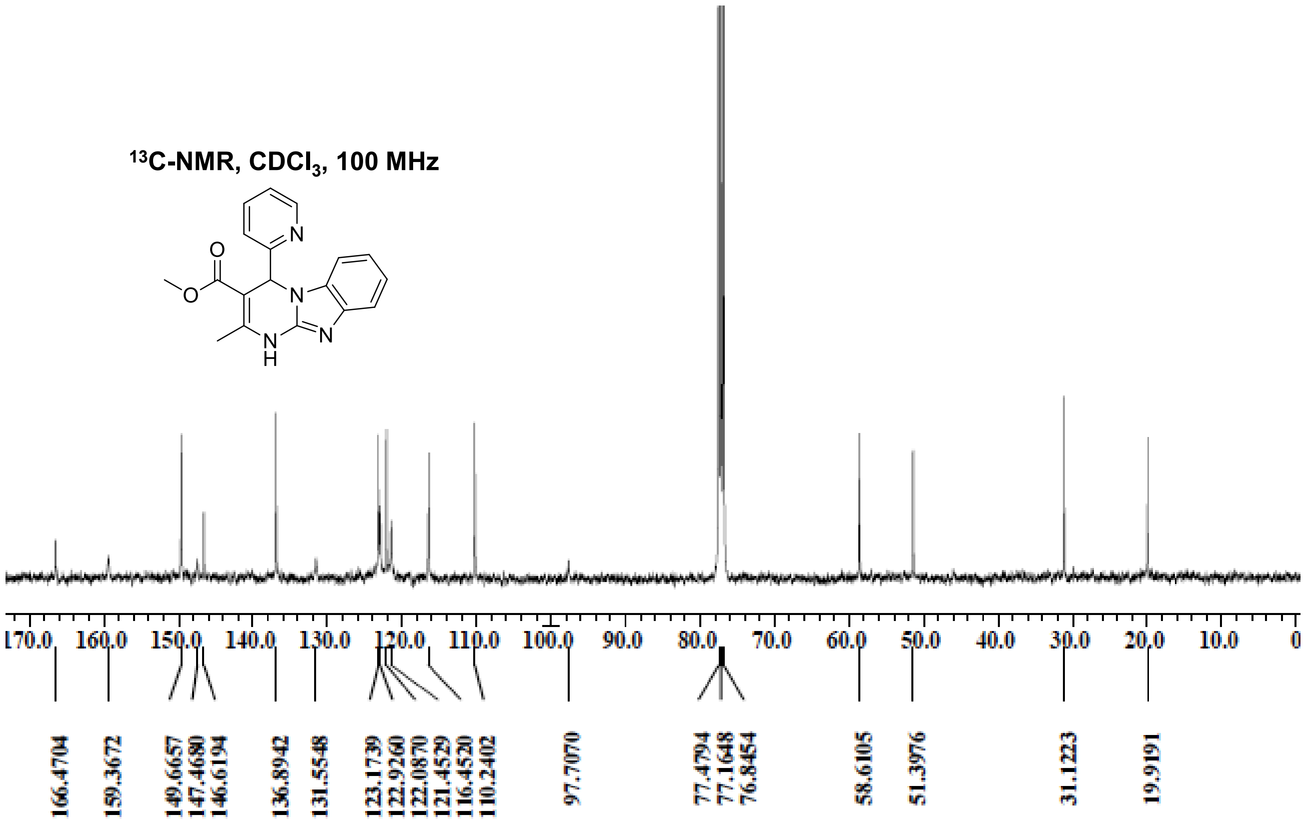

Figure S2. ^{13}C NMR spectrum of compound **1**.

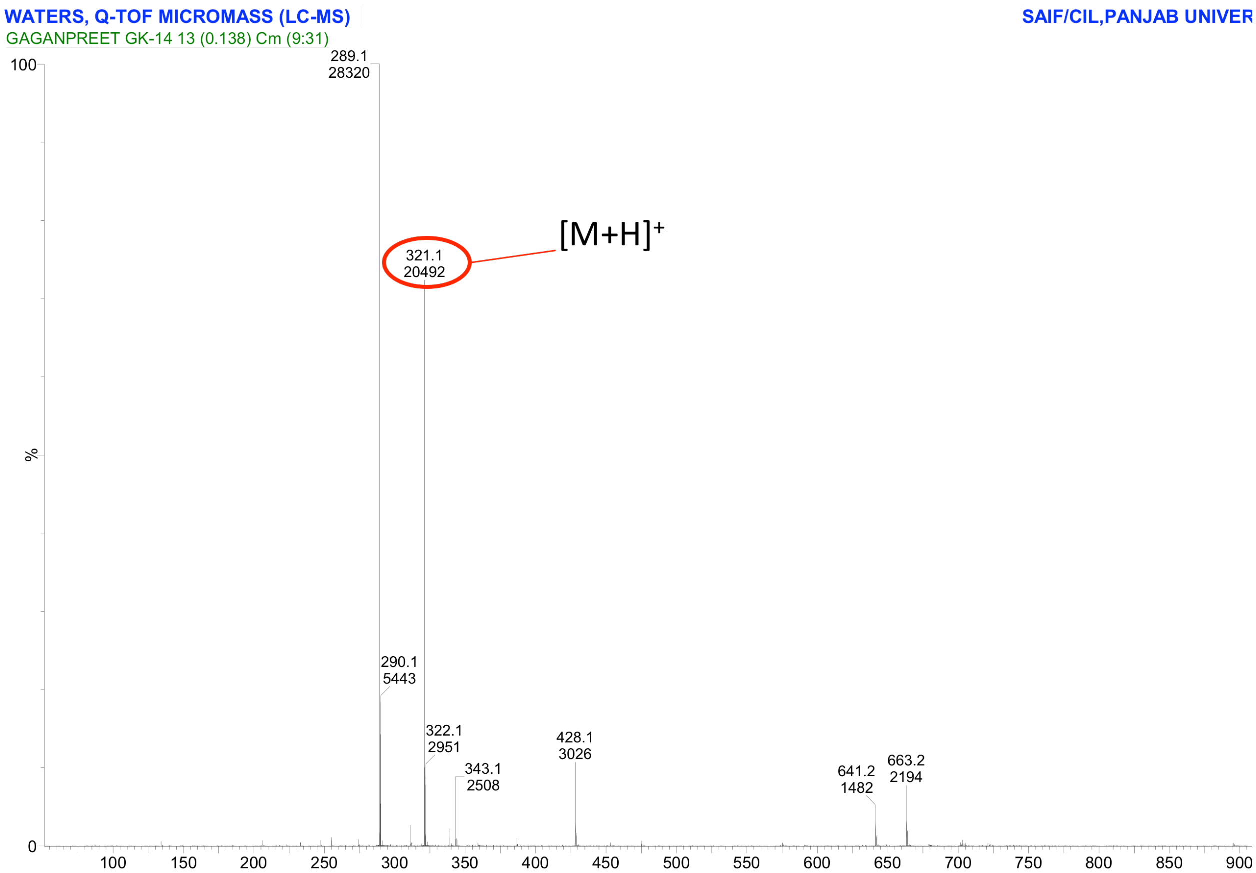

Figure S3. ESI Mass spectrum of compound **1**.

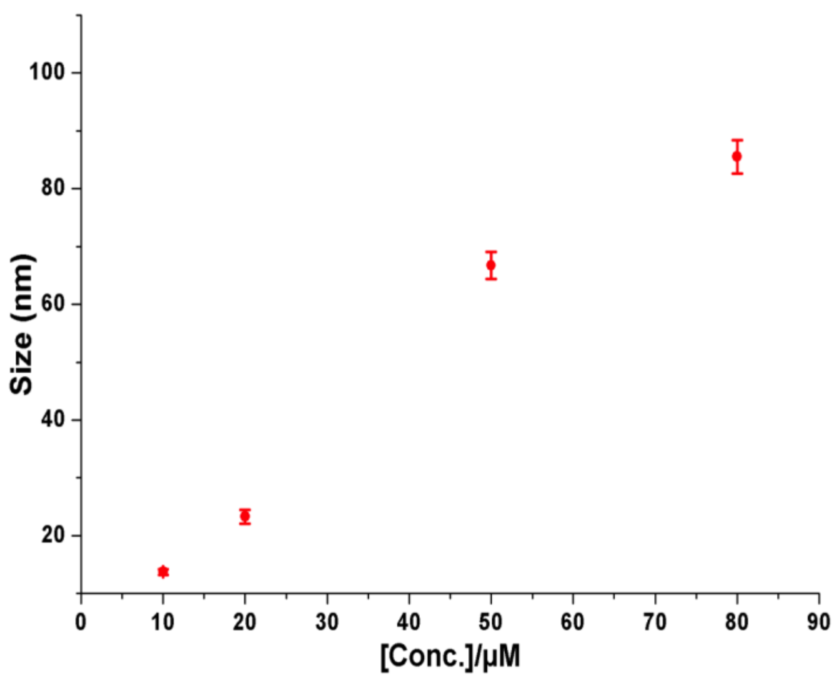

Figure S4. Plot of variation in size of nanoparticles as a function of concentration of compound **1** in water.

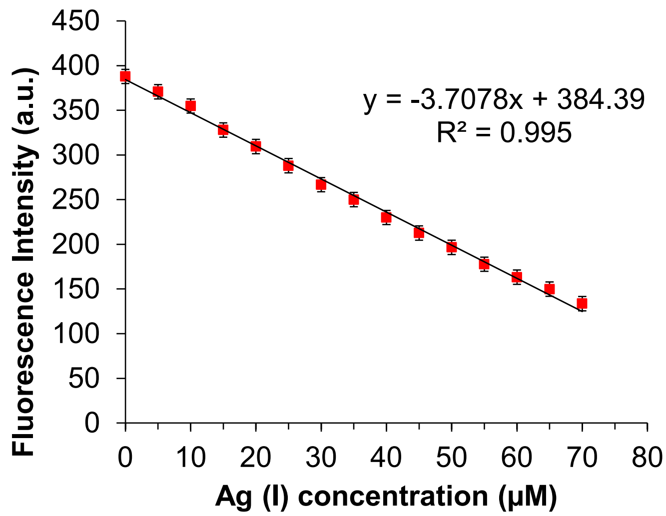

Figure S5. Linear regression graph for Ag (I) titration.

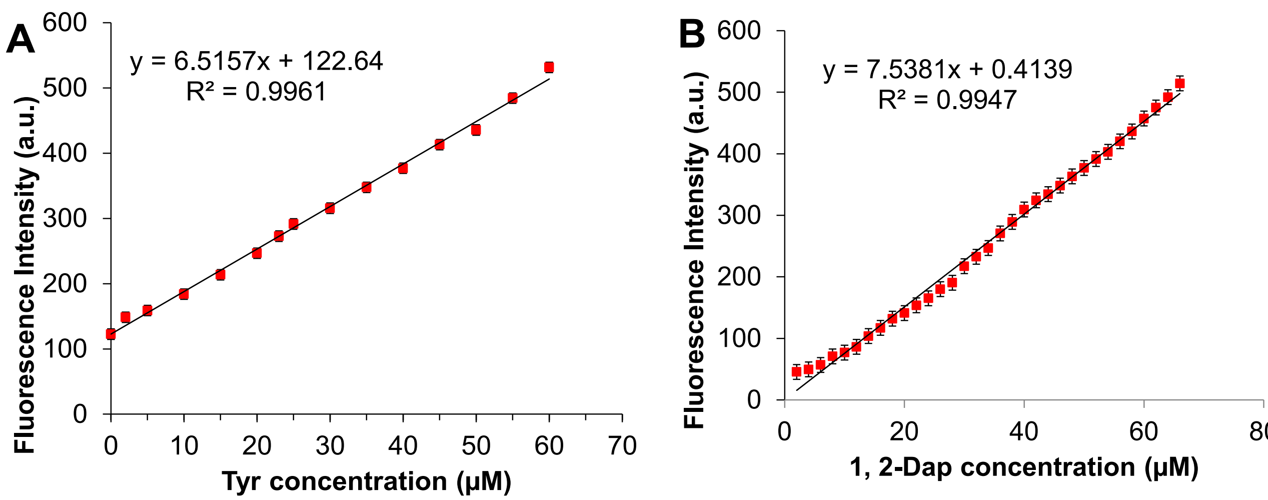

Figure S6. Linear regression graphs for Tyramine titration (A) and linear regression graph for 1,2-Diaminopropane titration (B).

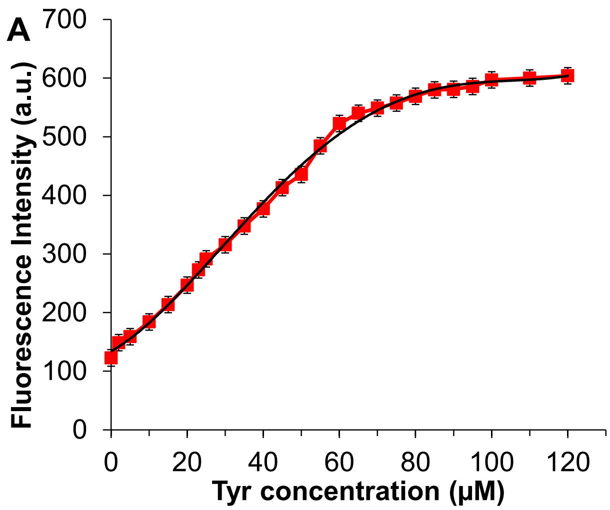

Figure S7. Non-linear regression graphs between Fluorescence Intensity vs. Concentrations of amines (at higher concentrations).

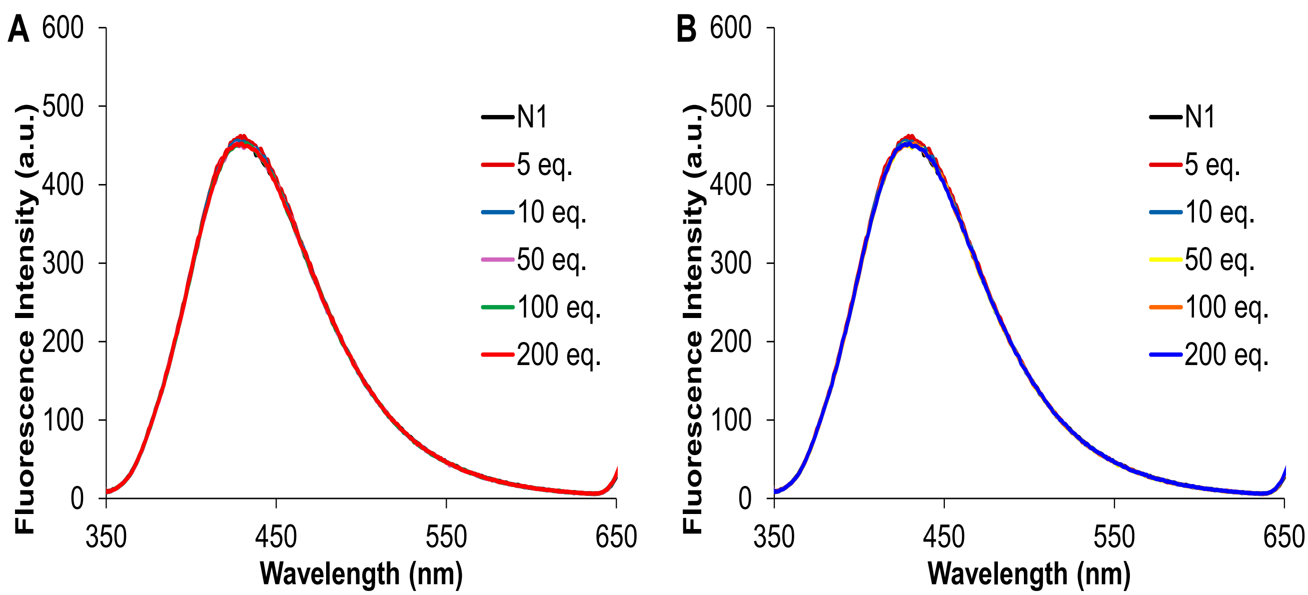

Figure S8. Fluorescence spectra of nano-aggregates **N1** at different concentrations of (A) TBA perchlorate to evaluate the salt effect and (B) in presence of NaCl.

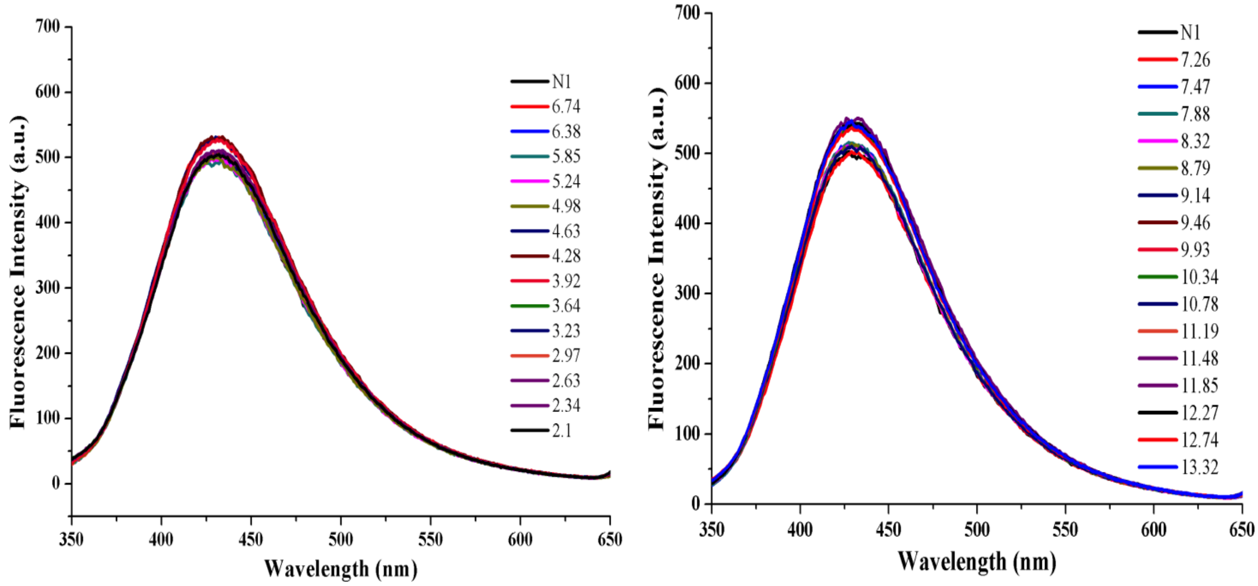

Figure S9. Fluorescence spectra of nano-aggregates **N1** at different pH values.

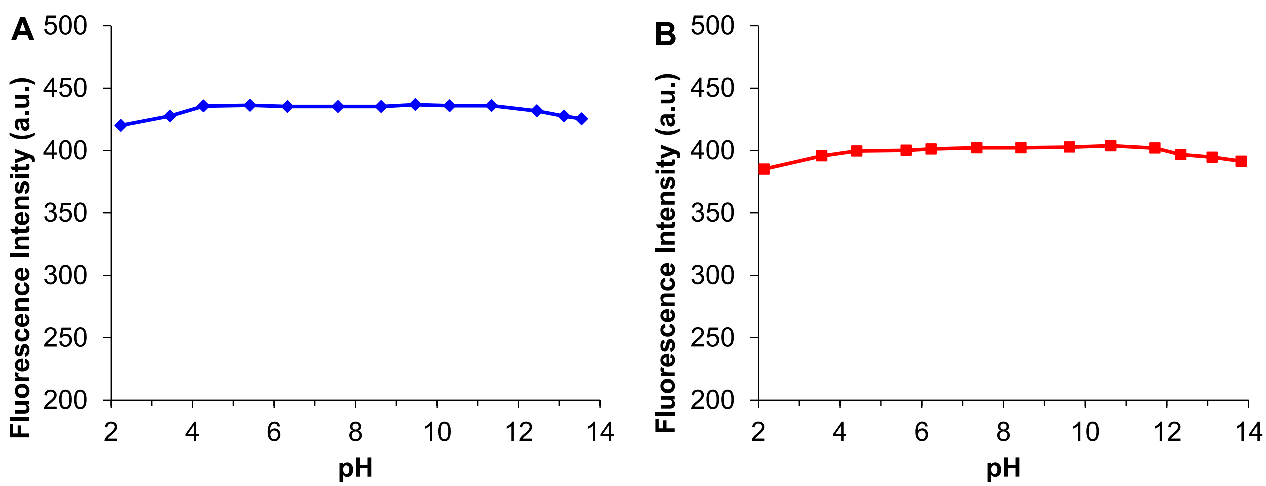

Figure S10. Fluorescence intensity v/s pH graphs of A) **N1.Ag(I)** complex with 50 μM Tyramine and B) **N1.Ag(I)** complex with 50 μM 1,2-Diaminopropane.

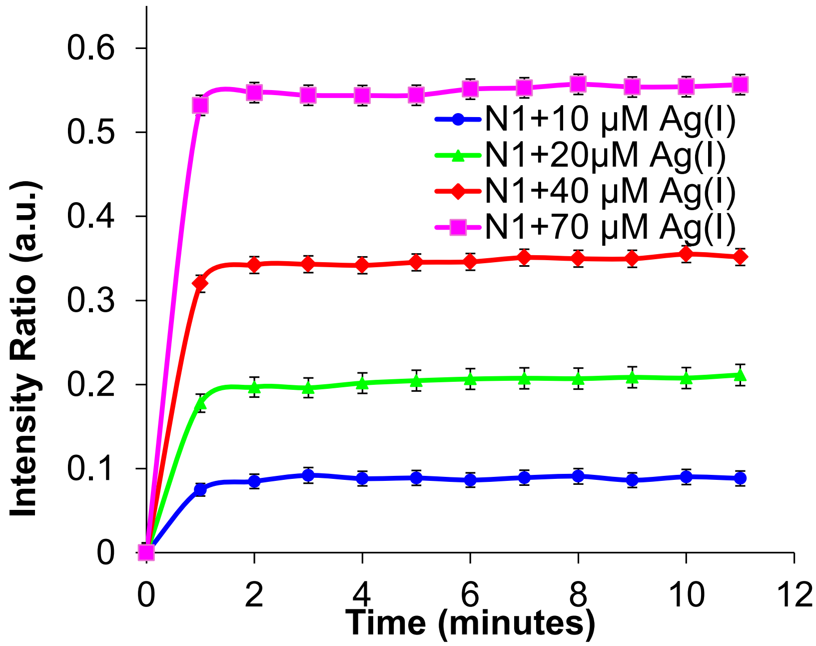

Figure S11. Plot of fluorescence intensity ratios of **N1** and Ag (I) at different concentrations, as a function of time.

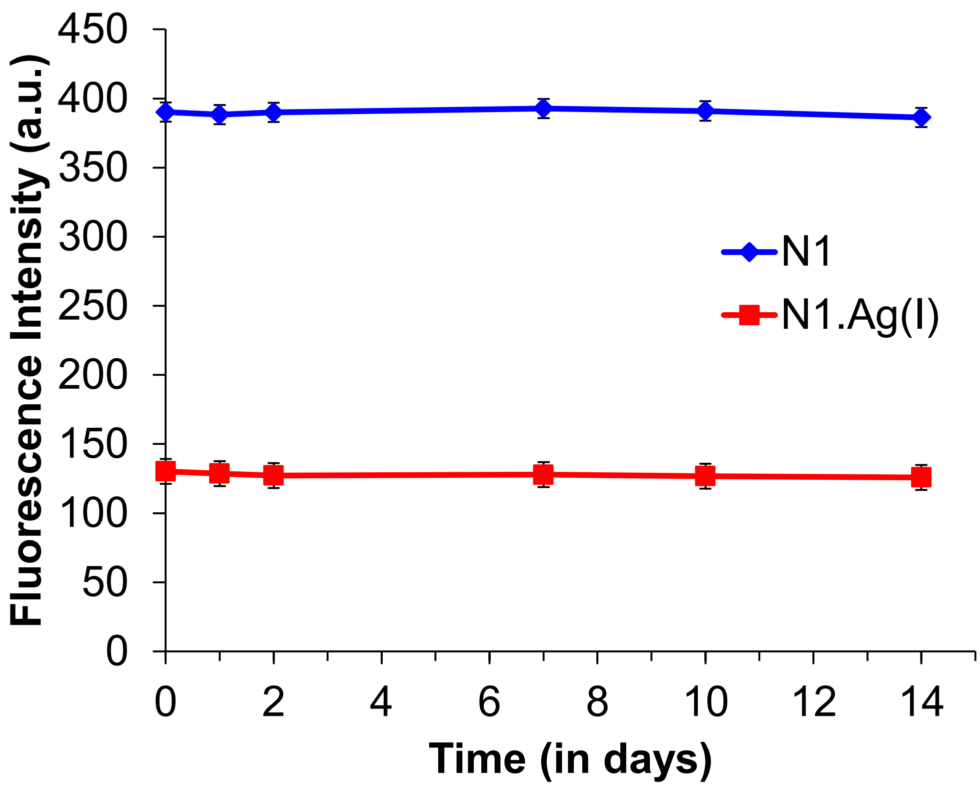

Figure S12. Stability of organic nanoparticles, **N1** and the **N1.Ag(I)** complex over a period of two weeks.

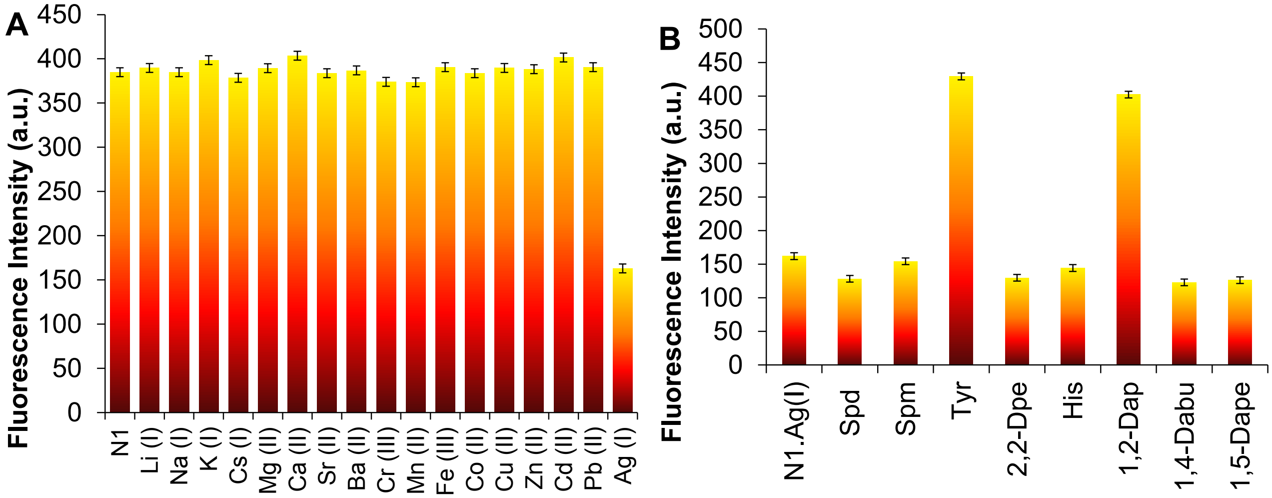

Figure S13. Fluorescence intensity variation of A) **N1** on addition of different metal ions and B) **N1.Ag(I)** on addition of different Biogenic amines using five different batches of sensors to check the reproducibility.

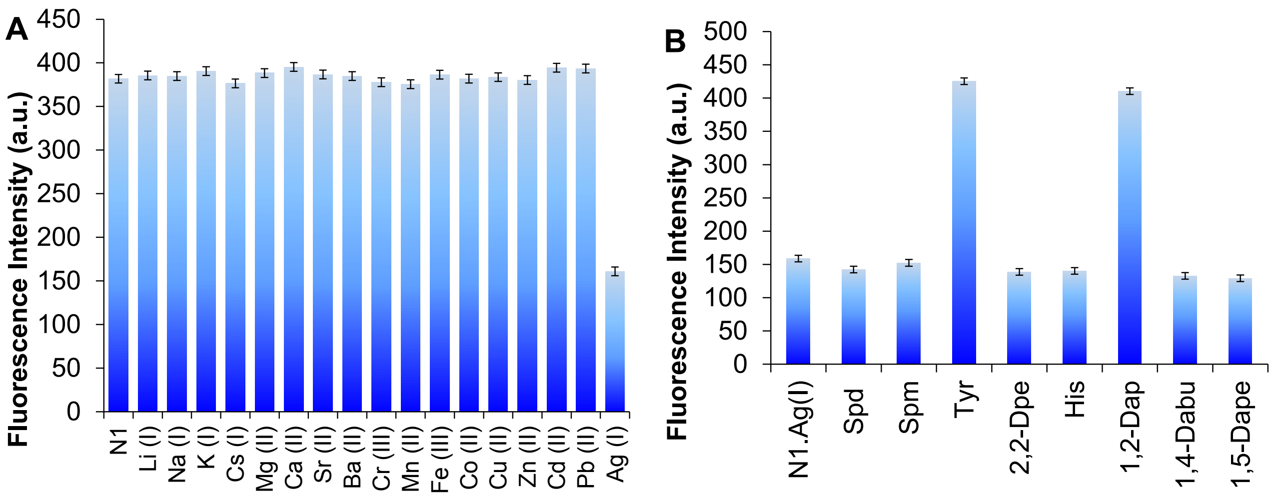

Figure S14. Fluorescence intensity variation of A) **N1** on addition of different metal ions and B) **N1.Ag(I)** on addition of different Biogenic amines in presence of HEPES buffer, pH 7.4.

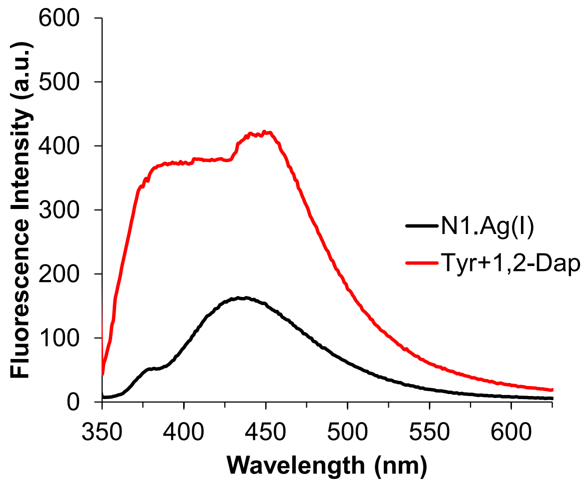

Figure S15. Fluorescence intensity v/s wavelength graph of **N1.Ag(I)** complex with 50 μM each of Tyramine and 50 μM 1,2-Diaminopropane mixed together.

Determination of detection limit.

The detection limit (DL) of nano-aggregates of **1** for Ag (I) was determined from the following equation:

$$DL = \frac{KS_{b1}}{S}$$

Where K = 3; S_{b1} is the standard deviation of the blank solution; S is the slope of the calibration curve. The detection limits of biogenic amines were also determined in a similar fashion.

Table S1: Comparison of current sensor with existing literature.

S. No.	Mode of detection	Pretreatment	Application to real sample analysis	Detection limit	Reference
1	UV	Pretreatment	Urine	0.06 µM	*J. Sep. Sci.*, 2009, **32**, 4143–4147.
2	Matrix -solid -phase-dispersion using HPLC −electrospray−tandem MS	Pretreatment	Cheese	0.06 mg/kg	*J. Agric. Food Chem*. 2005, **53**, 3779−3783.
3	UHPLC-MS/MS	Pretreatment	Anchovy (fish)	Range: 10−750 µg/L	*J. Agric. Food Chem*. 2012, **60**, 5324−5329
4	RP-HPLC coupled with fluorimetry	precolumn dansylation	Wines	0.04 mg/l	*Food Chem*., 2008, **106**, 1218–1224
5	Electrochemical sensor based on MWCNT-gold nanoparticle composites	-	Yoghurt	57 nM	*Food Res. Int*., 2011, **44**, 276–281.
6	Cyclic voltammetry using SWCNT	Pretreatment	Fish products	0.62 µM	*J. Food Eng*., 2015, **149**, 1–8.
7	Absorption-based Chromogenic Sensing on filter paper	-	-	0.02 mM	*Anal. Chem*. 2010, **82**, 8402-8405
8	Chameleon dye based, microtitre plate using fluorescence spectroscopy	Pretreatment	Fish samples	3.4 µM	*Analyst*, 2011, **136**, 4492–4499
9	Micellar liquid chromatography and pulsed amperometric	-	Wine	12ng/ml	*J. Chromatogr. A*, 2007, **1156**, 288–295.
10	Amperometry	Pretreatment	Sauerkraut	0.57 µM	*Sens. Actuators B*, 2013, **178**, 40– 46
11	Fluorescence Spectroscopy-using easily-engineered nanomaterials	No	Milk and Wine	3.91 nM	Current study.